Journal of *Fungi*

MDPI

Article

Characterization of the Growth and Morphology of a BSL-2 *Coccidioides posadasii* Strain That Persists in the Parasitic Life Cycle at Ambient CO_2

Javier A. Garcia [1], Kiem Vu [1], George R. Thompson III [2,3] and Angie Gelli [1,*]

[1] Department of Pharmacology, School of Medicine, University of California, Davis, CA 95616, USA; jagarc@ucdavis.edu (J.A.G.); kbvu@ucdavis.edu (K.V.)
[2] Department of Medicine, Division of Infectious Diseases, University of California, Davis, CA 95616, USA; grthompson@ucdavis.edu
[3] Department of Medical Microbiology and Immunology, University of California, Davis, CA 95616, USA
* Correspondence: acgelli@ucdavis.edu; Tel.: +1-530-219-0743

Abstract: *Coccidioides* is a dimorphic fungus responsible for Valley Fever and is the cause of severe morbidity and mortality in the infected population. Although there is some insight into the genes, pathways, and growth media involved in the parasitic to saprophytic growth transition, the exact determinants that govern this switch are largely unknown. In this work, we examined the growth and morphology of a *Coccidioides posadasii* strain (*C. posadasii* S/E) that efficiently produces spherules and endospores and persists in the parasitic life cycle at ambient CO_2. We demonstrated that *C. posadasii* S/E remains virulent in an insect infection model. Surprisingly, under spherule-inducing conditions, the *C. posadasii* S/E culture was found to be completely hyphal. Differential interference contrast (DIC) and transmission electron microscopy (TEM) revealed unexpected cellular changes in this strain including cell wall remodeling and formation of septal pores with Woronin bodies. Our study suggests that the *C. posadasii* S/E strain is a useful BSL-2 model for studying mechanisms underlying the parasitic to saprophytic growth transition—a morphological switch that can impact the pathogenicity of the organism in the host.

Keywords: *Coccidioides*; *Galleria mellonella*; hyphal growth; spherules

Citation: Garcia, J.A.; Vu, K.; Thompson, G.R., III; Gelli, A. Characterization of the Growth and Morphology of a BSL-2 *Coccidioides posadasii* Strain That Persists in the Parasitic Life Cycle at Ambient CO_2. *J. Fungi* **2022**, *8*, 455. https://doi.org/10.3390/jof8050455

Academic Editor: Aaron Neiman

Received: 29 March 2022
Accepted: 26 April 2022
Published: 28 April 2022

1. Introduction

Dimorphic fungi are major causes of fungal disease, particularly due to their adapted life cycles in the environment and the host. *Coccidioides* is a major cause of pulmonary disease in the arid southwestern United States where the disease manifests in patients' lungs and can disseminate to the skin, bones, and central nervous system [1,2]. Infection begins when arthroconidia are inhaled from exposure sites in endemic areas. Although *Coccidioides*' parasitic life cycle has been largely characterized by the spherule/endospore (SE) phase in the host, much less is known about its hyphal morphologies in vivo.

Coccidioides posadasii and *Coccidioides immitis* are two known species responsible for coccidioidomycosis, an opportunistic fungal infection that causes significant morbidity and mortality in endemic areas [1,3]. Although located in arid and semi-arid regions of the United States, the exact distribution of *Coccidioides* in the soil is difficult to determine, even in endemic areas [4]. Furthermore, the factors that favor growth in the environment and within the host remain largely unknown. Increasing concentrations of greenhouse gases and rising temperatures promote *Coccidioides*' thermotolerance and survival in the environment—traits that can help the organism adapt to growth in a human host [3–5].

Previous studies have used global transcriptomics to examine differentially expressed genes in the saprophytic (hyphal) and parasitic (spherule/endospore) life cycles [6,7]. However, the exact mechanisms underlying the morphological switch remain elusive.

Here, we examine the growth dynamics, morphology, and ultrastructure of a strain of *Coccidioides posadasii* (*C. posadasii* S/E) that persists in the parasitic life cycle in Converse media at ambient CO_2, but switches to saprophytic growth (hyphal morphology) in media that mimics an in vivo-like environment, a phenomenon not expected based on previous reports [8]. The characterization of the *C. posadasii* S/E strain that maintains its spherule/endospore life cycle under routine laboratory condition provides the *Coccidioides* research community with a model organism for studying the molecular factors that are active during the parasitic life cycle and the mechanisms underlying the parasitic to saprophytic growth transition—an important morphological change that has the potential to impact the pathogenicity of the organism.

2. Materials and Methods

2.1. Strains and Growth Conditions

A Silveira strain of *Coccidioides posadasii* was maintained in the spherule/endospore phase (parasitic phase) and approved by Biological Use Authorization for Biosafety Level 2 use. The strain was acquired from Dr. Pappagianis (UC Davis). *C. posadasii* spherules stored at −80 °C in 15% glycerol were inoculated into 150 mL of chemically defined Converse media. Converse media, prepared as previously described, contained potassium phosphate monobasic, zinc sulfate, calcium chloride dihydrate, sodium chloride, sodium bicarbonate, magnesium sulfate heptahydrate, ammonium acetate, dextrose, Tamol, and potassium phosphate dibasic trihydrate, filter-sterilized with 0.22 µM Stericup (Millipore, Burlington, MA, USA) and stored at room temperature [9,10]. Cultures were grown in vented flasks, incubated at 37 °C at ambient CO_2/O_2 and shaken at 160 rpm for up to 7 days as previously described [8]. The initial culture grown in Converse medium was sub-cultured into the respective test media by transferring 100µl aliquots of the initial culture to 150 mL of the respective test media. Roswell Park Memorial Institute-1640 (RPMI-1640) media (10.2 g/L) was supplemented with 10% heat-inactivated fetal bovine serum (FBS) (Life Technologies, Carlsbad, CA, USA) and 0.08% Tamol® (Dupont, USA, purchased from Northeastern Laboratories, Waterville, ME, USA) and filter-sterilized with 0.22 µM Stericup (Millipore) to create RPMI-sph media and stored at 4 °C for the continuous production of spherules and co-cultures with mammalian cell lines [8,11]. RPMI-tamol media contains only RPMI-1640 (10.2 g/L) and 0.08% Tamol® with no added FBS.

2.2. Galleria Mellonella Killing Assay

The *G. mellonella* killing assays were carried out as previously described but modified for *Coccidioides* [12,13]. Briefly, *G. mellonella* wax moth caterpillars (or larvae) (Vanderhorst, Inc., St. Marys, OH, USA) that were in the final instar stage were housed in the dark and used within 14 days from the day of shipment. Fourteen caterpillars of the desired weight (~245 mg +/− 25 mg) were used in all assays. The inocula were prepared as follows: *C. posadasii* S/E was grown for approximately 144 h in 100 mL of Converse media. The culture was centrifuged at 2000 rpm for 2 min and washed with 1× PBS three times. Cultures were visually inspected by light microscopy to ensure no contamination was present. Spherules were resuspended in 1× PBS, lightly mixed to break up cluster in order to accurately determine inoculum size and measured with a hemocytometer (Bright-Line™ Hemacytometer, Sigma-Aldrich, Burlington, MA, USA). Final concentrations of 1.25×10^3 and 1.25×10^5 cells/µL were prepared for injection. Before injection, the Hamilton syringe was cleaned sequentially with 10% bleach, 70% ethanol, and 1× PBS. Larvae were injected with 8 µL aliquots of the respective inoculum (10^4 and 10^6 total spherules per larvae) in the last left proleg (hemocoel) with the syringe. Injection area was cleaned with an ethanol swab and ampicillin (20 mg of ampicillin/kg of body weight) was co-administered to prevent contamination from native bacteria. Control larvae were injected with 8 µL of 1× PBS or heat-killed spherules of the same concentration. Spherules were inactivated by modifying a previous described procedure [14]. Briefly, aliquots were boiled in 100 °C water bath for 30 min and cell death was verified using 0.4% trypan blue solution (Millipore Sigma).

Larvae were incubated in 37 °C post-injection and monitored daily for survival. Graphs and statistical analysis were done with GraphPad Prism 5.0 statistical software (GraphPad, San Diego, CA, USA). Differences in survival (log rank and Wilcoxon tests) were analyzed by the Kaplan–Meier method. p values of <0.05 were considered significant [11].

2.3. Leica DIC DMRE Imaging

Cultures were grown in different media for 7 days in the 37 °C shaking incubator, washed with 1× PBS and fixed for one hour in 4% paraformaldehyde. Spherules were rinsed off with 1× PBS and mounted on a coverslip. Differential Interference Contrast (DIC) images were taken on a Leica DMRE microscope running MetaMorph v7.1. Images were processed on ImageJ. DIC images taken were also used to quantitatively compare spherule diameter in Converse and RPMI-tamol media. For the quantification of spherule diameter, ImageJ was calibrated with a micrometer (Reichert-Jung, Leica, Wetzlar, Germany) and values were recorded for each media condition. Sample size for each group was 30 spherules. Graphs and statistical analysis were done with GraphPad Prism statistical software using an unpaired t-test with Welch's correction (GraphPad, San Diego, CA, USA). p values of <0.05 were considered significant.

2.4. Enzymatic Release of Extracellular Proteins from S/E Phase Coccidioides

Spherules were harvested after 144–168 h and washed with phosphate-buffered saline (PBS). Spherule surface proteins were released in a 15 mL tube in triplicate by treating intact spherules with 3 mL of 0.25% trypsin/EDTA solution (Corning, Corning, NY, USA) for 4 h or 14 h at 37 °C and room temperature, respectively, on a rotating mixer. Following the trypsin treatment, the spherules were examined by compound light microscopy to ensure that they remained intact. Peptides resulting from the trypsin treatment were concentrated using a 3 kDa cutoff filter (Amicon, MilliporeSigma, Sigma Aldrich, St. Louis, MO, USA) and separated on an SDS-PAGE gel and visualized with Coomassie blue stain. For comprehensive trypsin digests, complete and concentrated samples were sequenced by LC-MS/MS.

2.5. Mass Spectrometry Sequencing

Supernatants from trypsinized cells and proteins bands of interest were excised from polyacrylamide gels and submitted to the UC Davis Proteomic Core. Scaffold4 (Proteome Software Inc., Portland, OR, USA) was used to validate MS/MS based peptide and protein identifications.

2.6. Transmission Electron Microscopy

Cultures were grown in Converse, RPMI-tamol, and RPMI-sph media for 7 days in the 37 °C shaking incubator, washed three times with 1× PBS and fixed in modified Karnovsky's fixative (2.5% glutaraldehyde, 2% paraformaldehyde in 0.1 M sodium phosphate buffer) overnight. Samples were submitted to the Biological Electron Microscopy Facility at University of California, Davis, for TEM sample preparation. Briefly, cells fixed overnight were centrifuged (2000 rpm for 3 min) to remove the fixative and rinsed in 0.1 M sodium phosphate buffer. Cells were then fixed in 1% osmium tetroxide/1.5% potassium ferrocyanide for 1 h and rinsed with cold water. Cells were dehydrated with 30%, 50%, 70%, 95%, and 100% (3 times) ethanol for 10 min each (7 total). Resin (Dodecenyl Succinic Anhydride, Araldite 6005, Epon 812, Dibutyl Phthalate, Benzyldimethylamine) was added and allowed to infiltrate cells overnight at room temperature. Fresh resin was added the next day and set to polymerize at 70 °C overnight. Polymerized blocks were sectioned on a Leica EM UC6 ultramicrotome at approximately 100 nm and collected on a copper grid. Grids were dried in 60 °C oven for 30 min and stained with 4% aqueous uranyl acetate and 0.4% lead citrate in 0.1 N NaOH. Sections were imaged with a TEM microscope (FEI Talos L120C TEM 80 kv) and images processed on ImageJ.

2.7. In Vitro Growth Kinetics

Fresh 150 mL of test media (Converse, RPMI-tamol, RPMI-sph) were inoculated with 100 µL of a 7-day initial S/E culture grown in Converse media. Cultures were visually inspected using light microscopy to ensure no contamination was present. Growth rates were determined by measuring OD_{600} and blanking the spectrophotometer with the respective media. Cultures were mixed prior to sampling to ensure settled cultures were homogenous. Measurements were taken in triplicate every 24 h for a period of 17 days starting at time zero. Light microscopy images were taken at the end of the 17 day incubation period to show a representation of the culture's morphology.

3. Results

3.1. C. posadasii S/E Spherules Are Virulent In Vivo

We investigated the virulence of *C. posadasii* S/E spherules in the *Galleria mellonella* insect model of infection. Survival of larvae infected with 10^4 live spherules was not different from larvae inoculated with PBS or with 10^4 heat-killed spherules (p = 0.7786) (Figure 1A). As the size of the inoculum could have varying effects on the larvae, we next challenged *G. mellonella* larvae with 10^6 spherules. At this inoculum size, we observed a statistically significant reduction in percent survival of larvae infected with live spherules compared to equal amounts of heat-killed spherules (p = <0.0001) or PBS-only control (p = <0.0001) (Figure 1B). Larvae challenged with 10^6 spherules succumbed to *C. posadasii* S/E within 4 days of infection (Figure 1B). On the other hand, 95% of larvae challenged with spherules that had been heat-killed were alive on day 4 and by the eighth day post-infection, 30% of animals survived (Figure 1B). The prolonged survival of larvae inoculated with heat-killed *C. posadasii* S/E spherules suggested only a limited role of proteins in the mechanism(s) of virulence.

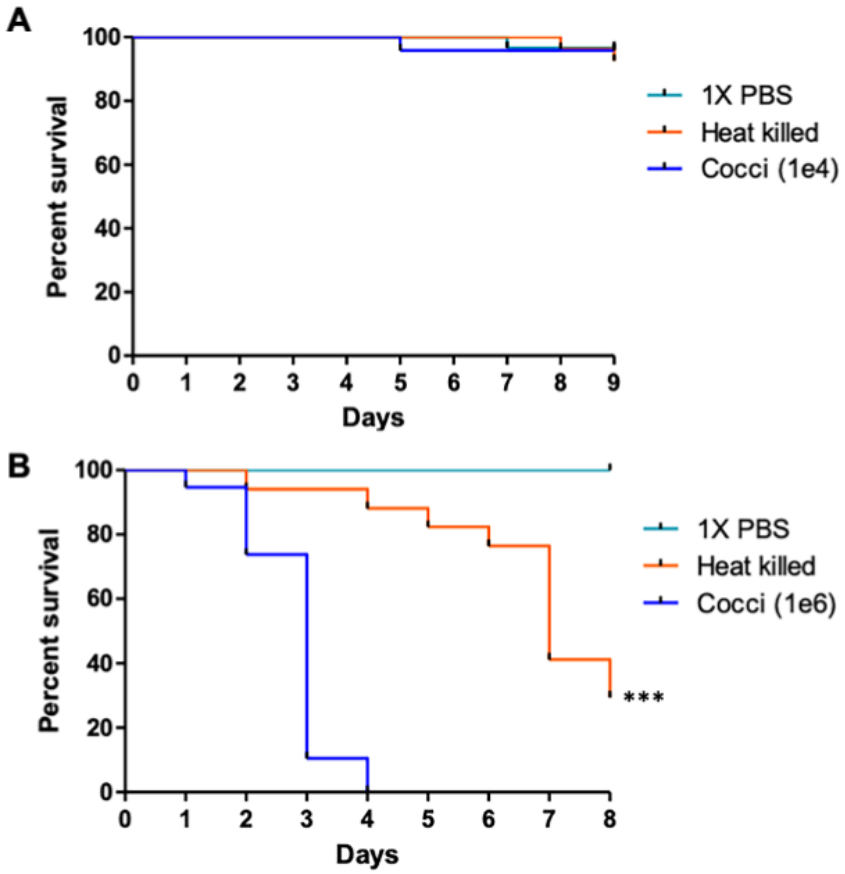

Figure 1. The *C. posadasii* S/E strain is virulent in an insect model of infection. Larva of *Galleria mellonella* inoculated with 10^4 spherules were not affected (**A**), whereas inoculation of 10^6 spherules

resulted in 100% death of larvae within 4 days (**B**). Heat-inactivation of the *C. posadasii* strain prior to inoculation improved survival significantly. PBS controls show no difference in survival. Statistical analysis was performed using GraphPad Prism software by estimating differences in survival (log rank and Wilcoxon tests) using the Kaplan–Meier method (*** $p = 0.0001$). Shown is one of three replicates.

3.2. Similarity in Surface Antigens of Coccidioides Identified in Human Chest Tissue and C. posadasii S/E Strain

To further assess the virulence of *C. posadasii* S/E, we evaluated the surface antigens of the spherules using a *Coccidioides*-specific monoclonal antibody (C-mAb) raised against a surface antigen. We found that C-mAb identified spherules in human chest tissue from a confirmed case of coccidioidomycosis (Figure 2, top panel). The C-mAb also stained the surface of *C. posadasii* S/E spherules that had been cultured and fixed (Figure 2, middle panel). The *Coccidioides*-specific mAb did not cross react with a reference strain of *Cryptococcus neoformans* (Figure 2, bottom panel), healthy human lung/chest tissue or diseased lung tissue (large cell carcinoma T2A N0 G3 tumors or squamous cell carcinoma) (data not shown). These results suggested that surface antigens of *C. posadasii* S/E spherules are likely similar to those found on spherules of *Coccidioides* isolates, consistent with the virulence of C. *posadasii* S/E in the *G. mellonella* model of infection.

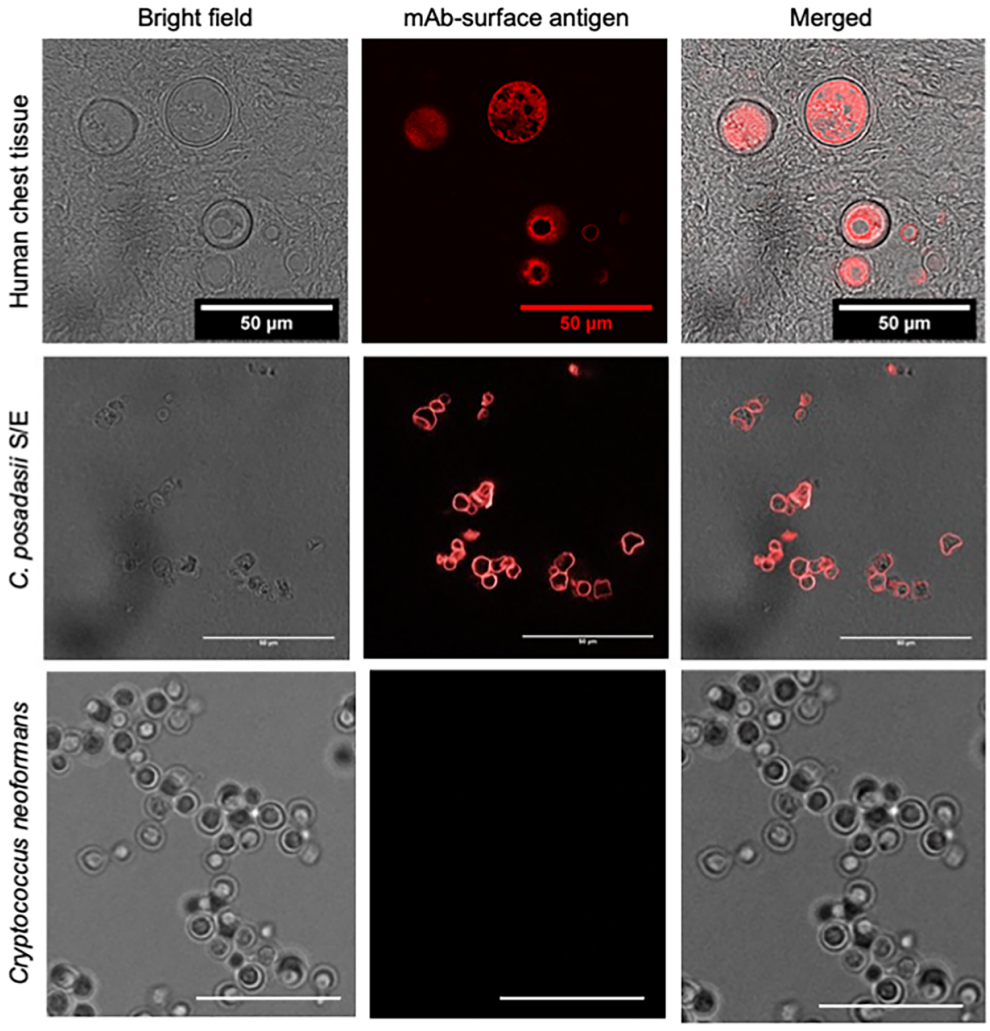

Figure 2. Surface antigen of *C. posadasii* S/E strain similar to *Coccidioides* identified in human chest tissue. (**Top** panel): IHC staining with a *Coccidioides* surface antigen mAb detects spherules in

human chest tissue with confirmed coccidioidomycosis. *Coccidioides* spherules were identified by brightfield imaging 10–30 µm. IHC staining using the *Coccidioides* mAb primary antibody and Alexa Fluor® 568 secondary antibody showed specific fluorescent signal localized on the surface of spherules (100× magnification). Brightfield and fluorescence images were merged and showed co-localization of spherules and fluorescent signal. (**Middle** panel): the same primary mAb used above stained the surface of *C. posadasii* S/E stain fixed with thimerosal. *Coccidioides* mAb primary antibody and Alexa Fluor® 568 secondary antibody showed specific fluorescent signal localized on the surface of spherules. (**Bottom** panel): *Coccidioides*-specific mAb did not cross react with the *Cryptococcus neoformans* KN99 reference strain (100× magnification, scale bar 25 µm).

We further examined the surface antigens of *C. posadasii* S/E spherules by identifying surface-exposed proteins. We isolated four highly abundant extracellular proteins by utilizing trypsin shaving of intact spherules from the cultured *C. posadasii* S/E strain and mass spectrometry for protein identification. Copper-zinc superoxide dismutase (SOD), DOMON-like type 9 carbohydrate binding module, aspartyl protease, and mannosyl-oligosaccharide alpha-1,2-mannosidase precursor were identified as surface proteins of *C. posadasii* S/E spherules (Table 1, Supplementary File S1). These same proteins were identified as immunoreactive antigens in other *Coccidioides* strains from previous studies [15–19].

Table 1. Immunoreactive proteins on the surface of *C. posadasii* S/E spherules. Surface proteins were isolated by Trypsin shaving of intact spherules, separated by SDS-PAGE electrophoresis and excised polypeptide band was identified by mass spectrometry.

Protein/Predicted Function	NCBI Protein Sequence ID (Accession Number)	Molecular Weight (kDa)	Number of Unique Peptides	Percent Coverage	References
Copper, zinc superoxide dismutase (SOD)	ABB36775.1 (C5P5N2_COCP7)	26	10	20	[15]
DOMON-like type 9 carbohydrate binding module	AEB21190.1 (C5PIH6_COCP7)	26	5	18	[16]
Aspartyl proteinase	QVM08509.1 (C5P9L1_COCP7)	44	3	11	[17,18]
Mannosyl-oligosaccharide alpha-1,2-mannosidase	E9CXX8.1$% (C5PAF0_COCP7)	57	2	5	[19]

3.3. *C. posadasii* S/E Reverts to Mycelial Form in the Spherule-Producing Media, RPMI-Sph

As expected, *C. posadasii* S/E produced spherules and endospores continuously and rapidly in Converse media at ambient CO_2/O_2 without initiating the culture from arthroconidia (Figure 3A, top panel). Prior work found that reference strains of *Coccidioides* continuously produced spherules when grown in RPMI-sph media—conditions similar to those found in vivo [6,9]. Therefore, we investigated whether *C. posadasii* S/E behaved similar to the reference strains in RPMI-sph. Surprisingly, we found that *C. posadasii* S/E reverted to a nearly 100% hyphal form without any observable arthroconidia after 7 days of culture in RPMI-sph (Figure 3A, bottom panel).

To identify the media component that may have contributed to the transition from parasitic (spherule/endospore) to saprophytic (environmental form) growth, we removed FBS from RPMI-sph to create RPMI-tamol. A mixture of both mature spherules and mycelia was observed when *C. posadasii* S/E was grown in RPMI-tamol (Figure 3A, middle panel). We also noted that *C. posadasii* S/E spherules from RPMI-tamol cultures were larger and consistently more heterogenous in size compared to those grown in Converse media (Figure 3B). Therefore, we asked whether there was a difference in the growth rate of *C. posadasii* S/E in the different media (Figure 3C). Robust growth was observed in

RPMI-sph relative to growth in Converse or RPMI-tamol. Among the three different media, *C. posadasii* S/E grew the slowest in RPMI-tamol (Figure 3C).

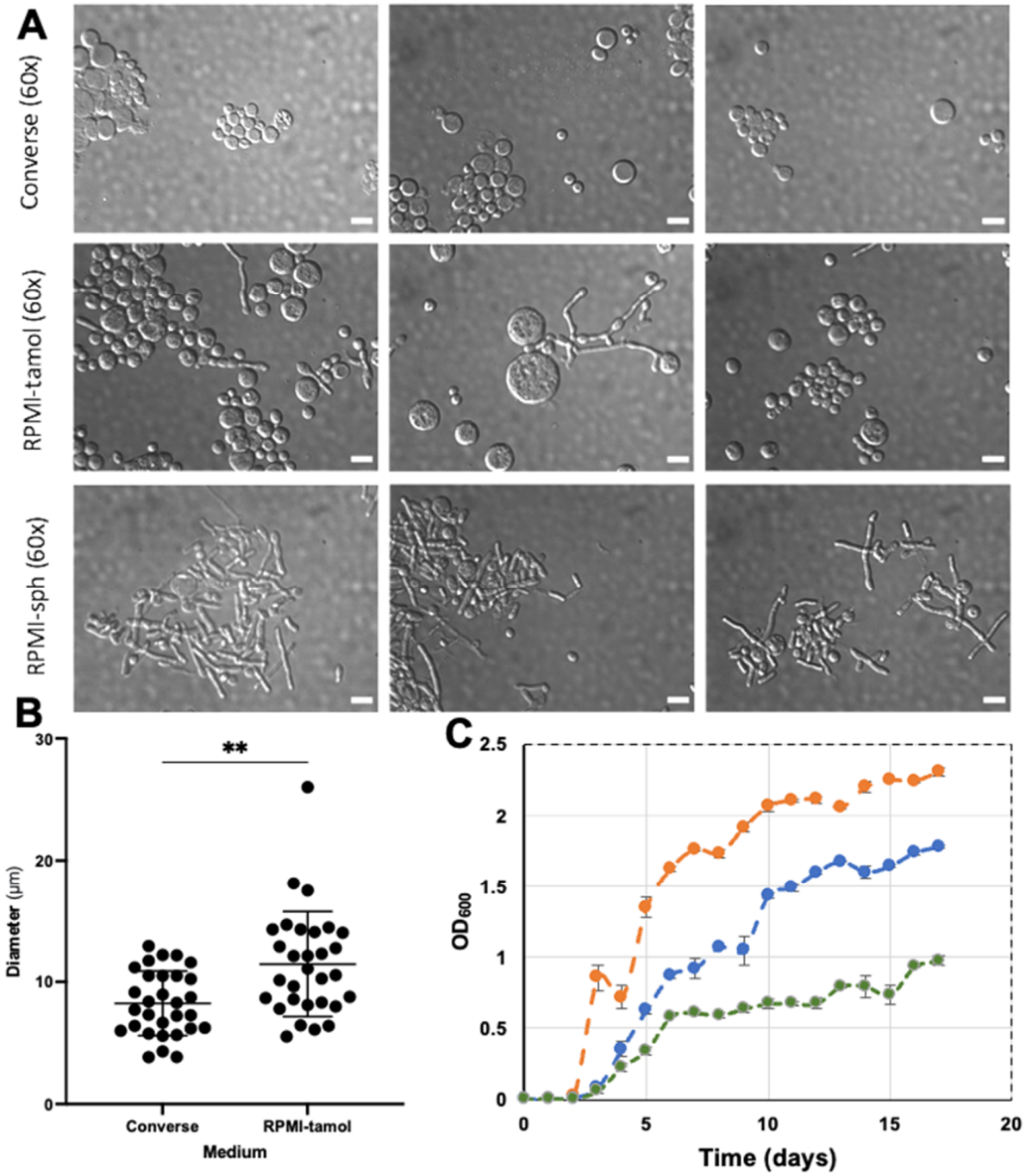

Figure 3. Differential Inference Contrast (DIC) microscope images show *C. posadasii* S/E morphology and size in different types of media. (**A**): Spherule and endospore production is optimal in Converse media. A mixture of spherule/endospores and hyphal morphologies are observed in RPMI-tamol media. Complete hyphal morphology is observed in RPMI-sph media. Images taken in triplicate on 60× magnification with Leica DMRE microscope. Scalebar represents 10 µm. (**B**): Spherules grown in RMPI-tamol are more varied and larger on average than spherules grown in Converse media. Graphs and statistical analysis were done using GraphPad Prism statistical software using an unpaired *t*-test with Welch's correction (** $p = 0.01$), n = 30. (**C**): The growth rates of the strain in three different mediums: Orange—RPMI-sph; Blue—converse media; and Green—RPMI-tamol.

3.4. Ultrastructural Features of C. posadasii S/E When Cultured in Different Media

The observed morphological changes of *C. posadasii* S/E in the different media prompted us to examine the ultrastructural features of the strain. Transmission electron microscopy (TEM) revealed enhanced endospore production in both Converse (Figure 4A) and RPMI-tamol media (Figure 4B) and very little spore production in RPMI-sph (Figure 4C). Mycelial cultures grown in RPMI-sph were largely devoid of endospores despite having a growth advantage over cultures grown in either Converse or RPMI-tamol. We also observed changes in the outer cell wall glycoprotein layer. TEM micrographs revealed that spherules grown in both Converse and RPMI-tamol had a loose outer cell wall layer that appeared to shed (Figure 4A,B). However, micrographs of mycelia grown in RPMI-sph showed a consistently smoother outer cell wall with minimal shedding (Figure 4C).

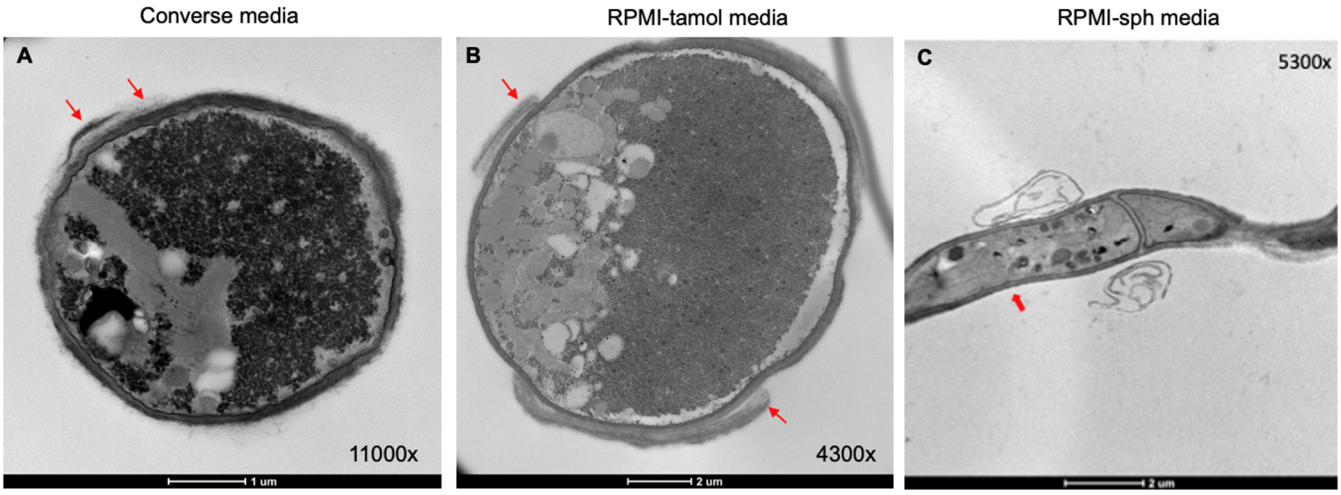

Figure 4. Ultrastructural features *of C. posadasii* S/E strain. TEM revealed a sloughing off of the outer cell wall glycoprotein layer of spherules (red arrows) grown in Converse (**A**) or RPMI-tamol media (**B**) that was not observed in the hyphal form ((**C**), red arrow). Hyphae also appeared to lack endospores in comparison to spherules. TEM images of *C. posadasii* S/E grown in Converse, RPMI-tamol, or RPMI-sph media were taken after 168 h growth in vitro.

The TEM studies also revealed that spherules grown in RPMI-tamol had ruffled, uneven cell walls. The most striking observation was the frequency of irregularly shaped spherules found in RPMI-tamol compared to the mostly round spherules observed in Converse media (Figure 5). Many spherules found in RPMI-tamol were elongated into an elliptical shape, and some appeared to be connected as pseudohyphae.

A closer look at the hyphae of *C. posadasii* S/E grown in either RPMI-tamol or RPMI-sph revealed a lack of endospores, as expected, and organelles such as mitochondria and nuclei were identified (Figure 6). The outer cell wall, inner wall, and plasma membrane were also clearly visible. Invaginations at the septum appeared to create a structure resembling a septal pore. The similarly sized organelles near the septal pores resembled Woronin bodies; these are small organelles used by filamentous ascomycetes to plug septal pores following an injury (Figure 6) [17].

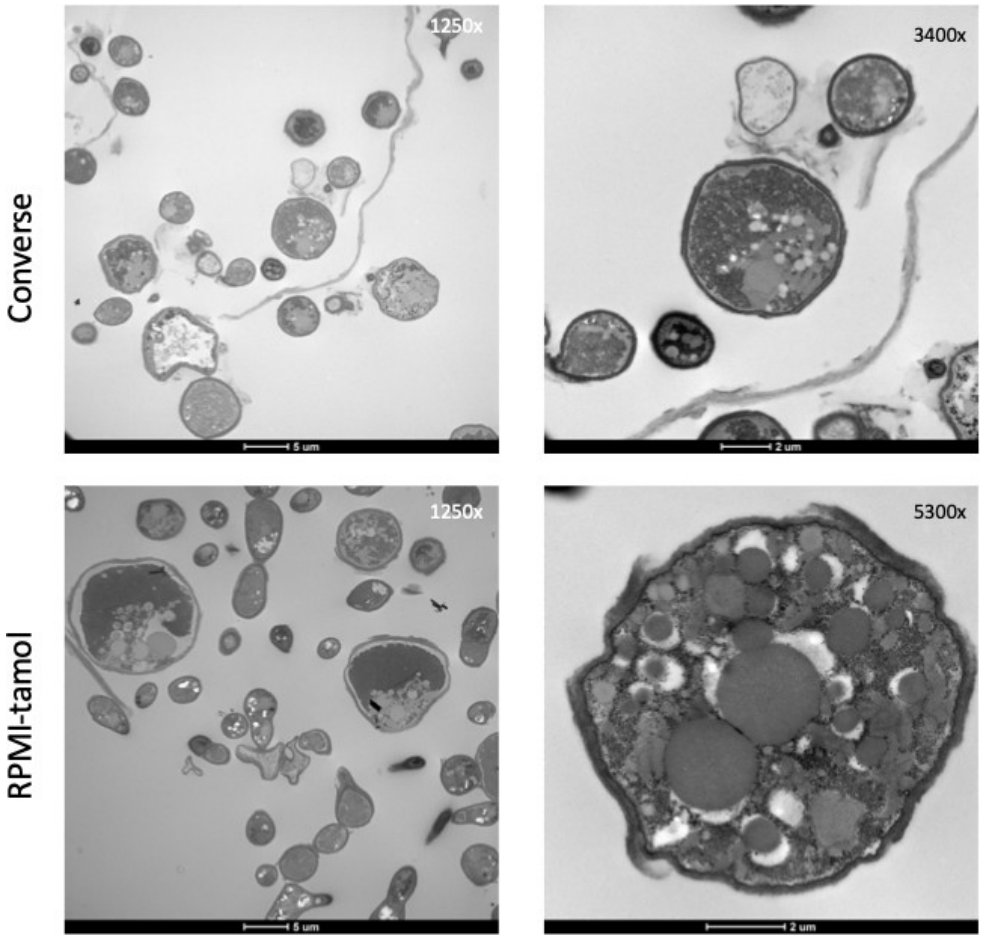

Figure 5. TEM images of *C. posadasii* S/E strain following 168 h growth in RPMI-tamol or Converse media. The shape of spherules grown in RPMI-tamol media are highly irregular compared to spherules grown in Converse media.

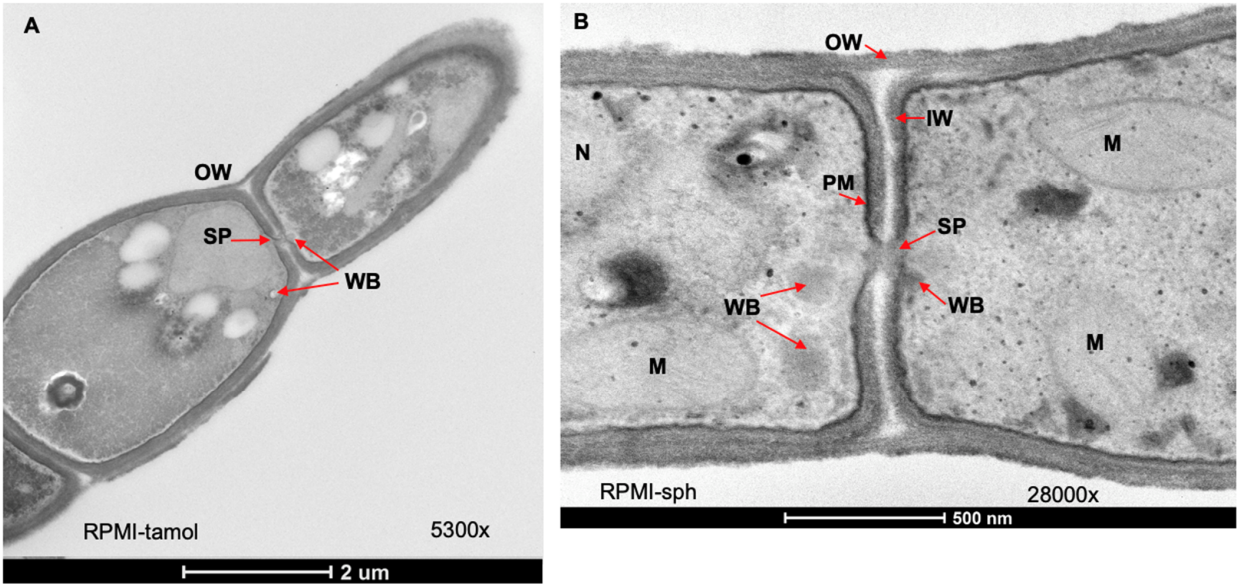

Figure 6. Hallmarks of mycelia observed in the mycelial form of *C. posadasii* S/E strain. TEM images of *C. posadasii* S/E strain following 168 h growth in RPMI-tamol (**A**) or RPMI-sph media

(**B**) SP: septal pore; WB: Woronin bodies; OW: outer wall; IW: inner wall; PM: plasma membrane; M: mitochondria; and N: nucleus.

4. Discussion

The aim of this study was to characterize a *C. posadasii* S/E strain and to establish whether it could serve as a useful BSL-2 model/tool for studies investigating the dimorphic transition of *Coccidioides*. Whereas reference strains of *Coccidioides* require 5–10% CO_2 for spherule induction in RPMI-sph, *C. posadasii* S/E could readily produce pure cultures containing spherules and endospores in Converse media at ambient CO_2/O_2 with no observable hyphae. Additionally, arthroconidia is not required to initiate *C. posadasii* S/E cultures, which can readily be started from a spherule glycerol stock. *C. posadasii* S/E has been approved by Biological Use Authorization for Biosafety Level 2 use because the strain strongly persists in the parasitic life cycle under routine laboratory conditions and there is low risk associated with unwanted sporulation. The availability of *C. posadasii* S/E for the research community would greatly facilitate future work on this under-studied human fungal pathogen due to the ease of producing large quantity of spherules for research and the ability to carry out studies under BSL-2 conditions.

Previous work utilized RPMI-containing media for the co-cultivation of both spherules and mammalian cell lines as well as the conversion of arthroconidia to spherules. A large body of literature has focused on the media composition that promotes the transition from saprophytic to parasitic growth as this morphological switch is important for the virulence of *Coccidioides* in the human host [7,9,18–27]. Significant differences in spherule density and size among various *Coccidioides* strains grown in RPMI-sph media were reported [6]. In contrast, *C. posadasii* S/E culture was found to be completely hyphal in RPMI-sph, and we did not observe new spherule formation even after 17 days of incubation. Rare spherules could be found in the RPMI-sph culture, but they likely originated from the initial inoculation used to start the culture.

Unlike the observed uniform mycelial culture of *C. posadasii* S/E in RPMI-sph, Mead et al. and Petkus et al. found both mycelia and spherules in RPMI-sph cultures of several *Coccidioides* strains [8,10]. Mycelia from cultures of *C. posadasii* C735, *C. posadasii* C735 Δ*cts2*/Δ*ard1*/Δ*cts3*, and *C. immitis* RMSCC 2006 could be detected at a later time (days 7–10); however, there was still significant spherule formation during this incubation period [8]. In contrast to the uniform mycelial morphology of *C. posadasii* S/E in RPMI-sph, *C. posadasii* S/E culture grown in RPMI-tamol had a mixture of both spherules and mycelia, and the spherules were significantly larger than those obtained from cultures grown in Converse media after 7 days of incubation. This result echoes the finding from the Mead et al. study in which spherules from wild-type *Coccidioides* strains were found to be larger in RPMI-tamol compared to those grown in Converse media. Together, our work and prior studies suggest that *C. posadasii* S/E behaves like a reference strain in RPMI-tamol [6] but, in RPMI-sph, *C. posadasii* S/E adopts a uniform hyphal morphology.

FBS is known to stimulate optimal hyphal growth of *Candida albicans* at 37 °C by downregulating a major regulator of hyphal morphogenesis, Ras1, suggesting that the Ras1-Cyr-PKA pathway might play a role in directing the life cycles of dimorphic fungi [20,21]. Furthermore, the Ras1-Cyr-PKA pathway is involved in activating the transcription factors Cph1 and Efg1, both of which are important for hyphal formation and activation of hyphal molecular switches in *C. albicans* [22].

Substantial evidence has documented the rare hyphal parasitic morphology of *Coccidioides* in several patients that present mycelial forms in tissues [23–29]. It is conceivable that the mycelial forms in the host could potentially be due to localized microenvironments created by low CO_2 conditions, cell-specific stimuli, or varying degrees of immunocompetence of the host [28,30]. This atypical hyphal form can complicate diagnosis as it could be confused with other filamentous fungal pathogens [31,32]. The *C. posadasii* S/E strain could potentially be used as a model organism for studying atypical *Coccidioides* morphology and developing diagnostic tools.

The growth rates of *C. posadasii* S/E varied significantly in different media. Cultivation of *Coccidioides* typically requires a long incubation period: 3–5 days to grow on plates, 6 weeks to harvest arthroconidia, and another 3–7 days to harvest spherules [7,8]. The *C. posadasii* S/E culture reached an OD_{600} of 0.8553 by day 3 in RPMI-sph, by day 6 in Converse, and by day 15–16 in RPMI-tamol. The different growth rates could potentially be attributed to the additional carbon source and nutrients from FBS. We found that the growth curve of the *C. posadasii* S/E culture was atypical and characterized by fast changes in optical density, likely as a result of nutrient exhaustion and nutrient shifting. It has been noted that several filamentous ascomycetes including *Penicillium ochrochloron*, *Trichoderma harzianium*, *Aspergillus niger*, and *Aspergillus nidulans* have similar growth curves that do not follow the classical logarithmic growth followed by a stationary phase [33]. On average, the cultures continued to increase in optical density over time; however, the higher OD could result from media evaporation due to long incubation (17 days) at 37 °C.

The virulence of *C. posadasii* S/E was assessed in the *Galleria mellonella* insect model. The insect model is advantageous as an in vivo model of infection due to its cost effectiveness and ease of handling and viability assessment [12,34,35]. Currently, there are no published studies that have used *G. mellonella* as a model of infection for *Coccidioides*, particularly with spherules as the inoculum. *C. posadasii* S/E spherules were found to significantly reduce survival of *Galleria mellonella* larvae over time. We did not see a reduction in survival when larvae were inoculated with 10^4 spherules, a comparable inoculum size used in our prior studies investigating the virulence of *Cryptococcus neoformans* [13]. Increasing the number of spherules to 10^6 resulted in 100% death of larvae, consistent with previous work showing that the spherule/endospore phase is less virulent than arthroconidia in murine models of infection [36]. The *Galleria mellonella* larvae inoculated with heat inactivated *C. posadasii* S/E showed an improvement in survival, however the continued killing of larvae by the heat-inactivated strain suggested only a limited role of proteins in the mechanism(s) of virulence. Other molecules in the spherules that were thermo-tolerant or potentially the by-products of thermo-inactivated small molecules/metabolites could be responsible for the toxic effects in the larvae.

Performing the *G. mellonella* studies with only the *C. posadasii* S/E strain was a limitation of the study. As a BSL-2 strain, we performed these experiments under BSL-2 conditions, which greatly facilitated our work. However, due to constraints that prevented us from utilizing BSL-3 facilities, we could not work with a reference strain of *Coccidioides* [8]. Additional studies will be needed to examine the virulence of *C. posadasii* S/E spherules together with reference strains such as the parent strain *C. posadasii* Silveira, *C. posadasii* C735, *C. immitis* RS, and *C. immitis* 2006 [8]. Another BSL-2 strain that warrants further comparison is *C. posadasii* Δ*cts2*/Δ*ard1*/Δ*cts3*—a mutant with the *C. posadasii* C735 background that produces sterile spherules incapable of endosporulation in the parasitic phase and is avirulent in mice [37]. Future work utilizing mycelia from *C. posadasii* S/E grown in RPMI-sph should also be evaluated to determine if pre-conditioning *C. posadasii* S/E in RPMI-sph has a significant effect on its pathogenicity.

As hyphae, *C. posadasii* S/E produced little to no endospores in the culture. Some hyphae appeared to grow as a pseudohyphae in RPMI-sph while others formed septa. We were the first to image and document septal pores in the saprophytic phase of *Coccidioides*. Septal pores allow the movement of organelles from cell to cell. When cells detect damage, Woronin bodies block septal pores to prevent the loss of organelles and other cellular contents essential for cell survival [38]. We were able to identify Woronin-like bodies near the septal pore, consistent with prior work showing Woronin-like bodies near the septum using electron microscopy [39]. Our data also lends support to the study by Whiston et al. which found that Hex1, a gene responsible for the formation of Woronin bodies, was upregulated in mycelia [7]. Several studies have shown that Hex1-homolog mutants in other filamentous fungi including *Aspergillus fumigatus*, *Arthrobotrys oligospora*, *Metarhizium robertsii*, and *Verticillium dahlia* have reduced virulence in their respective host [40–43].

Deactivating the Woronin-body stress response to injury could potentially be used as an anti-virulence mechanism to treat infections caused by mycelial forms in the host.

Spherules grown in either Converse or RPMI-tamol media have a constant shedding of the outer wall as previously observed in the reference *Coccidioides* C375 strain, suggesting that *C. posadasii* S/E spherules retain phenotypes similar to reference strains of *C. posadasii* under these growth conditions [44,45]. However, examination of mycelia formed in RPMI-sph showed that the outer wall remained intact with minimal shedding. Interestingly, Mead et al. found that spherules of *C. posadasii* C735 Δ*cts2*/Δ*ard1*/Δ*cts3* had thick and intact cell walls, similar to what we found with mycelia of *C. posadasii* S/E [44]. The pathway involving *cts2*/*ard1*/*cst3* is therefore likely downregulated in *C. posadasii* S/E when cultured in RPMI-sph and likely crucial for cell wall remodeling.

In summary, we report the characterization of a *Coccidioides posadasii* (*C. posadasii* S/E) strain that can serve as a useful BSL-2 model for studying the complex molecular changes involved in the life cycle transition in response to specific stimuli.

Supplementary Materials: The following supporting information can be downloaded at: https://www.mdpi.com/article/10.3390/jof8050455/s1, File S1: Sequence identity and peptide sequences of spherule-surface proteins.

Author Contributions: Conceptualization, A.G., J.A.G., K.V. and G.R.T.III; methodology, A.G., J.A.G., K.V. and G.R.T.III; formal analysis, J.A.G., K.V. and A.G.; resources, G.R.T.III; data curation, J.A.G. and K.V.; and writing—original draft preparation and editing to final manuscript: J.A.G., K.V., A.G. and G.R.T.III; All authors have read and agreed to the published version of the manuscript.

Funding: This research was funded by NIH T32 HL007013 Training in Comparative Lung Biology and Medicine.

Institutional Review Board Statement: Not applicable.

Informed Consent Statement: Not applicable.

Data Availability Statement: Not applicable.

Acknowledgments: We are grateful to the members of the Gelli Lab for their insightful discussions. We thank the UC Davis Biological Electron Microscopy Facility staff for the processing of samples for TEM and the Proteomics Core Facility at UC Davis. We thank the UC Davis Center for Valley Fever for sharing reagents, equipment and assistance. J.A.G. was supported by the NIH T32 HL007013 Training in Comparative Lung Biology and Medicine.

Conflicts of Interest: The authors declare no conflict of interest. The funders had no role in the design of the study; in the collection, analyses, or interpretation of data; in the writing of the manuscript; or in the decision to publish the results.

References

1. Stockamp, N.W.; Thompson, G.R., III. Coccidioidomycosis. *Infect. Dis. Clin. N. Am.* **2016**, *30*, 229–246. [CrossRef] [PubMed]
2. Van Dyke, M.C.C.; Thompson, G.R.; Galgiani, J.N.; Barker, B.M. The Rise of Coccidioides: Forces Against the Dust Devil Unleashed. *Front. Immunol.* **2019**, *10*, 2188. [CrossRef] [PubMed]
3. Brown, J.; Benedict, K.; Park, B.J.; Thompson, G.R., III. Coccidioidomycosis: Epidemiology. *Clin. Epidemiol.* **2013**, *5*, 185–197. [CrossRef] [PubMed]
4. Ocampo-Chavira, P.; Eaton-Gonzalez, R.; Riquelme, M. Of Mice and Fungi: *Coccidioides* spp. Distribution Models. *J. Fungi* **2020**, *6*, 320. [CrossRef]
5. Garcia-Solache, M.A.; Casadevall, A. Global warming will bring new fungal diseases for mammals. *mBio* **2010**, *1*, e00061-10. [CrossRef]
6. Mitchell, N.M.; Sherrard, A.; Dasari, S.; Magee, D.M.; Grys, T.; Lake, D.F. Proteogenomic Re-Annotation of Coccidioides posadasii Strain Silveira. *Proteomics* **2018**, *18*, 1700173. [CrossRef]
7. Whiston, E.; Wise, H.Z.; Sharpton, T.; Jui, G.; Cole, G.T.; Taylor, J.W. Comparative transcriptomics of the saprobic and parasitic growth phases in Coccidioides spp. *PLoS ONE* **2012**, *7*, e41034. [CrossRef] [PubMed]
8. Mead, H.L.; Teixeira, M.M.; Galgiani, J.N.; Barker, B.M. Characterizing in vitro spherule morphogenesis of multiple strains of both species of Coccidioides. *Med. Mycol.* **2019**, *57*, 478–488. [CrossRef]
9. Converse, J.L.; Besemer, A.R. Nutrition of the Parasitic Phase of Coccidioides Immitis in a Chemically Defined Liquid Medium. *J. Bacteriol.* **1959**, *78*, 231–239. [CrossRef]

10. Petkus, A.F.; Baum, L.L.; Ellis, R.B.; Stern, M.; Danley, D.L. Pure spherules of Coccidioides immitis in continuous culture. *J. Clin. Microbiol.* **1985**, *22*, 165–167. [CrossRef]
11. Lee, C.Y.; Iii, G.R.T.; Hastey, C.J.; Hodge, G.C.; Lunetta, J.; Pappagianis, D.; Heinrich, V. Coccidioides Endospores and Spherules Draw Strong Chemotactic, Adhesive, and Phagocytic Responses by Individual Human Neutrophils. *PLoS ONE* **2015**, *10*, e0129522. [CrossRef] [PubMed]
12. Mylonakis, E.; Moreno, R.; El Khoury, J.B.; Idnurm, A.; Heitman, J.; Calderwood, S.B.; Ausubel, F.M.; Diener, A. Galleria mellonella as a model system to study Cryptococcus neoformans pathogenesis. *Infect. Immun.* **2005**, *73*, 3842–3850. [CrossRef] [PubMed]
13. Vu, K.; Gelli, A. Astemizole and an analogue promote fungicidal activity of fluconazole against Cryptococcus neoformans var. grubii and Cryptococcus gattii. *Med. Mycol.* **2010**, *48*, 255–262. [CrossRef]
14. Mead, H.L.; Blackmon, A.V.; Vogler, A.J.; Barker, B.M. Heat Inactivation of Coccidioides posadasii and Coccidioides immitis for Use in Lower Biosafety Containment. *Appl. Biosaf.* **2019**, *24*, 123–128. [CrossRef] [PubMed]
15. Lunetta, J.M.; Simmons, K.A.; Johnson, S.M.; Pappagianis, D. Molecular cloning and expression of a cDNA encoding a *Coccidioides posadasii* Cu,Zn superoxide dismutase identified by proteomic analysis of the coccidioidal T27K vaccine. *Ann. N. Y. Acad. Sci.* **2007**, *1111*, 181–197. [CrossRef] [PubMed]
16. Lunetta, J.M.; Pappagianis, D. Identification, molecular characterization, and expression analysis of a DOMON-like type 9 carbohydrate-binding module domain-containing protein of Coccidioides posadasii. *Med. Mycol.* **2014**, *52*, 591–609. [CrossRef]
17. Johnson, S.M.; Kerekes, K.M.; Zimmermann, C.R.; Williams, R.H.; Pappagianis, D. Identification and cloning of an aspartyl proteinase from Coccidioides immitis. *Gene* **2000**, *241*, 213–222. [CrossRef]
18. Tarcha, E.J.; Basrur, V.; Hung, C.Y.; Gardner, M.J.; Cole, G.T. A recombinant aspartyl protease of Coccidioides posadasii induces protection against pulmonary coccidioidomycosis in mice. *Infect. Immun.* **2006**, *74*, 516–527. [CrossRef]
19. Lunetta, J.M.; Simmons, K.A.; Johnson, S.M.; Pappagianis, D. Molecular cloning and expression of a cDNA encoding a Coccidioides posadasii 1,2-alpha-mannosidase identified in the coccidioidal T27K vaccine by immunoproteomic methods. *Ann. N. Y. Acad. Sci.* **2007**, *1111*, 164–180. [CrossRef]
20. Ahmed, R.; Kodgire, S.; Santhakumari, B.; Patil, R.; Kulkarni, M.; Zore, G. Serum responsive proteome reveals correlation between oxidative phosphorylation and morphogenesis in Candida albicans ATCC10231. *J. Proteom.* **2018**, *185*, 25–38. [CrossRef]
21. Feng, Q.; Summers, E.; Guo, B.; Fink, G. Ras signaling is required for serum-induced hyphal differentiation in Candida albicans. *J. Bacteriol.* **1999**, *181*, 6339–6346. [CrossRef] [PubMed]
22. Martin, R.; Moran, G.P.; Jacobsen, I.D.; Heyken, A.; Domey, J.; Sullivan, D.J.; Kurzai, O.; Hube, B. The Candida albicans-specific gene EED1 encodes a key regulator of hyphal extension. *PLoS ONE* **2011**, *6*, e18394. [CrossRef] [PubMed]
23. Fee, H.J.; McAvoy, J.M.; Michals, A.A.; Gold, P.M. Unusual manifestation of Coccidioides immitis infection. *J. Thorac. Cardiovasc. Surg.* **1977**, *74*, 548–550. [CrossRef]
24. Fiese, M.J.; Cheu, S.; Sorensen, R.H. Mycelial forms of Coccidioides immitis in sputum and tissues of the human host. *Ann. Intern. Med.* **1955**, *43*, 255–270. [CrossRef] [PubMed]
25. Puckett, T.F. Hyphae of Coccidioides immitis in tissues of the human host. *Am. Rev. Tuberc.* **1954**, *70*, 320–327. [CrossRef]
26. Putnam, J.S.; Harper, W.K.; Greene, J.F., Jr.; Nelson, K.G.; Zurek, R.C. Coccidioides immitis. A rare cause of pulmonary mycetoma. *Am. Rev. Respir. Dis.* **1975**, *112*, 733–738. [CrossRef]
27. Thadepalli, H.; Salem, F.A.; Mandal, A.K.; Rambhatla, K.; Einstein, H.E. Pulmonary mycetoma due to Coccidioides immitis. *Chest* **1977**, *71*, 429–430. [CrossRef]
28. Dolan, M.J.; Lattuada, C.; Melcher, G.; Zellmer, R.; Allendoerfer, R.; Rinaldi, M. Coccidioides immitis presenting as a mycelial pathogen with empyema and hydropneumothorax. *J. Med. Vet. Mycol.* **1992**, *30*, 249–255. [CrossRef]
29. Munoz-Hernandez, B.; Martinez-Rivera, M.A.; Palma Cortes, G.; Tapia-Diaz, A.; Manjarrez Zavala, M.E. Mycelial forms of Coccidioides spp. in the parasitic phase associated to pulmonary coccidioidomycosis with type 2 diabetes mellitus. *Eur. J. Clin. Microbiol. Infect. Dis.* **2008**, *27*, 813–820. [CrossRef]
30. Munoz-Hernandez, B.; Palma-Cortes, G.; Cabello-Gutierrez, C.; Martinez-Rivera, M.A. Parasitic polymorphism of Coccidioides spp. *BMC Infect. Dis.* **2014**, *14*, 213. [CrossRef]
31. Kaufman, L.; Valero, G.; Padhye, A.A. Misleading manifestations of Coccidioides immitis in vivo. *J. Clin. Microbiol.* **1998**, *36*, 3721–3723. [CrossRef]
32. Hagman, H.M.; Madnick, E.G.; D'Agostino, A.N.; Williams, P.L.; Shatsky, S.; Mirels, L.F.; Tucker, R.M.; Rinaldi, M.G.; Stevens, D.A.; Bryant, R.E. Hyphal forms in the central nervous system of patients with coccidioidomycosis. *Clin. Infect. Dis.* **2000**, *30*, 349–353. [CrossRef] [PubMed]
33. Vrabl, P.; Schinagl, C.W.; Artmann, D.J.; Heiss, B.; Burgstaller, W. Fungal Growth in Batch Culture-What We Could Benefit If We Start Looking Closer. *Front. Microbiol.* **2019**, *10*, 2391. [CrossRef]
34. Fuchs, B.B.; Chaturvedi, S.; Rossoni, R.D.; de Barros, P.P.; Torres-Velez, F.; Mylonakis, E.; Chaturvedi, V. Galleria mellonella experimental model for bat fungal pathogen Pseudogymnoascus destructans and human fungal pathogen Pseudogymnoascus pannorum. *Virulence* **2018**, *9*, 1539–1547. [CrossRef]
35. Trevijano-Contador, N.; Zaragoza, O. Immune Response of Galleria mellonella against Human Fungal Pathogens. *J. Fungi* **2018**, *5*, 3. [CrossRef]
36. Clemons, K.V.; Capilla, J.; Stevens, D.A. Experimental animal models of coccidioidomycosis. *Ann. N. Y. Acad. Sci.* **2007**, *1111*, 208–224. [CrossRef]

37. Xue, J.; Chen, X.; Selby, D.; Hung, C.-Y.; Yu, J.-J.; Cole, G.T. A genetically engineered live attenuated vaccine of Coccidioides posadasii protects BALB/c mice against coccidioidomycosis. *Infect. Immun.* **2009**, *77*, 3196–3208. [CrossRef]
38. Jedd, G.; Chua, N.H. A new self-assembled peroxisomal vesicle required for efficient resealing of the plasma membrane. *Nat. Cell Biol.* **2000**, *2*, 226–231. [CrossRef]
39. Cutler, J.E.; Erke, K.H. Ultrastructural characteristics of Coccidioides immitis, a morphological variant of Cryptococcus neoformans and Podosypha ravenelii. *J. Bacteriol.* **1971**, *105*, 438–444. [CrossRef]
40. Beck, J.; Ebel, F. Characterization of the major Woronin body protein HexA of the human pathogenic mold Aspergillus fumigatus. *Int. J. Med. Microbiol.* **2013**, *303*, 90–97. [CrossRef]
41. Beck, J.; Echtenacher, B.; Ebel, F. Woronin bodies, their impact on stress resistance and virulence of the pathogenic mould Aspergillus fumigatus and their anchoring at the septal pore of filamentous Ascomycota. *Mol. Microbiol.* **2013**, *89*, 857–871. [CrossRef]
42. Liang, L.; Gao, H.; Li, J.; Liu, L.; Liu, Z.; Zhang, K.-Q. The Woronin body in the nematophagous fungus Arthrobotrys oligospora is essential for trap formation and efficient pathogenesis. *Fungal Biol.* **2017**, *121*, 11–20. [CrossRef]
43. Tang, G.; Shang, Y.; Li, S.; Wang, C. MrHex1 is Required for Woronin Body Formation, Fungal Development and Virulence in Metarhizium robertsii. *J. Fungi* **2020**, *6*, 172. [CrossRef]
44. Mead, H.L.; Roe, C.C.; Keppler, E.A.H.; Van Dyke, M.C.C.; Laux, K.L.; Funke, A.; Miller, K.J.; Bean, H.D.; Sahl, J.W.; Barker, B.M. Defining Critical Genes During Spherule Remodeling and Endospore Development in the Fungal Pathogen, Coccidioides posadasii. *Front. Genet.* **2020**, *11*, 483. [CrossRef]
45. Hung, C.Y.; Yu, J.J.; Seshan, K.R.; Reichard, U.; Cole, G.T. A parasitic phase-specific adhesin of Coccidioides immitis contributes to the virulence of this respiratory Fungal pathogen. *Infect. Immun.* **2002**, *70*, 3443–3456. [CrossRef]